Rock-magnetic and paleomagnetic survey on dated lava flows erupted during the Bruhnes and Matuyama chrons: the Mascota Volcanic Field revisited (Western Mexico)

RAFAEL GARCÍA-RUIZ[1], AVTO GOGUITCHAICHVILI[1], MIGUEL CERVANTES-SOLANO[2], JUAN MORALES[1], RAFAEL MACIEL-PEÑA[3], JOSÉ ROSAS-ELGUERA[4], RUBEN CEJUDO-RUIZ[1] AND JAIME URRUTIA-FUCUGAUCHI[1]

1 Laboratorio Interinstitucional de Magnetismo Natural, Instituto de Geofisica, Unidad Michoacan, Universidad Nacional Autonoma de México, Campus Morelia, 58190 Morelia, México (rafaelgr@geofisica.unam.mx)

2 Escuela Nacional de Estudios Superiores (ENES), Unidad Morelia, Universidad Nacional Autonoma de México, Campus Morelia, 58190 Morelia, México

3 Instituto Tecnológico Superior de Tacámbaro, División de Investigación y Estudios Profesionales, Av. Tecnológico 201, Tacámbaro Michoacán 61650, México

4 Laboratorio Interinstitucional de Magnetismo Natural, Sede Guadalajara, Universidad de Guadalajara, México

Received: June 3, 2016; Revised: November 30, 2016; Accepted: January 2, 2017

ABSTRACT

A rock magnetic and paleomagnetic investigation was performed on some selected, radiometrically dated lava flows from the Mascota Volcanic Field (MVF), western Trans-Mexican Volcanic Belt. A set of rock-magnetic experiments and standard paleomagnetic analysis were carried out on 19 sites spanning the time interval from 2268 to 72 kyr. The paleomagnetic directions are anchored to absolute radiometric ages while no such information was available in previous studies. This makes possible to correctly evaluate the fluctuation of Earth's magnetic field from Pliocene to Pleistocene and reveal the firm evidence of possible Levantine excursion. Both Ti-poor and Ti-rich titanomagnetites seem to carry the remanent magnetization with Curie temperatures ranging from 350°C to 537°C. Thirteen flows correspond to the Brunhes chron, one of them exhibits transitional directions, while the remaining six sites belong to the Matuyama chron. New and existing dataset for MVF were used to estimate the paleosecular variation parameters. The selected data include 35 Plio-Quaternary lava flows. After excluding the poor quality data, as well as the transitional directions, the mean paleodeclination is 356.1° and oaleoinclination 39.9°, which agree well with the geocentric axial dipole (GAD) and the expected paleodirections for the Plio-Pleistocene, as derived from the reference poles for the stable North America. The corresponding mean paleomagnetic poles are paleolongitude 226.7° and paleolatitude 86.0°. The virtual geomagnetic pole scatter for

the MVF is 15.2°, which is consistent with the value expected from model G at latitude of 20° (this model provides an interpretation of the paleosecular variation at different latitudes for the time of interest). The combined paleomagnetic data, supported by positive reversal test, indicate no paleomagnetically detectable vertical-axis rotations in the study area. The evidence of one transitional directions was detected, which may correspond to the Levantine excursion (360-370 kyr) or unnamed event between 400–420 kyr.

Keywords: Mascota volcanic field, paleosecular variation, Plio-Quaternary, geocentric axial dipole, Western Mexico

1. INTRODUCTION

Main paleomagnetic applications are based on the geocentric axial dipole (GAD) hypothesis that provides a coordinate reference frame over long-time scales. Paleomagnetic studies for the past 5 Myr essentially support the GAD, showing that more than 90% of paleofield power corresponds to the geocentric axial dipole. Present and paleofield studies also indicate the presence of higher order structures (*Merril and McElhinny, 1985*; *Johnson and Constable, 1995,1998*). Many studies confirm that the GAD is a first order approximation but some anomalous spatial-temporal paleosecular variation (PSV) patterns were also documented (*Wilson, 1972*; *Wilson and McElhinny, 1974*; *Schneider and Kent, 1990*). Zonal and latitudinal-dependent PSV models have been developed during the last decades which permit to constraint PSV characteristics and persistent non dipole anomalies. Some studies also underlined the occurrence of regional PSV anomalies such as the Pacific dipole window and other minor PSV patterns characterized by low secular variation rates (*McElhinny et al., 1996*). PSV analyses at low latitudes, e.g., at ±20°N (the case of Central Mexico and Hawaii) have reported contrasting results. *Lawrence and Constable (2006)* have concluded that low PSV and smaller persistent GAD anomalies has characterized the low latitude zone during the Brunhes chron.

Volcanic rocks are reliable paleomagnetic recorders of the Earth's magnetic field because of high stability of the thermoremanent magnetization (e.g., *Prévot et al., 1985*). In ideal case, the PSV and GAD studies should rely on paleomagnetic data from radiometrically dated volcanic rocks. Volcanic data represent sporadic measurements, and thus time varying studies are limited by the number of paleomagnetic directions. Central México is characterized by stratovolcanoes and volcanic monogenetic fields that form the Trans-Mexican Volcanic Belt (TMVB). TMVB is an arc built on the continental margin related to plate subduction at the Middle America trench and presents large arc parallel variation in volcanic style (*Ferrari, 2000*).

The present study is aimed to increase high quality paleomagnetic data from the Jalisco Block adding nineteen radiometrically dated sites (*Ownby et al., 2008*). These new results permit to increase the robustness of existing (*Maillol and Bandy, 1993*; *Maillot et al., 1997*) data from the region during the Pliocene trough Pleistocene. The combined paleomagnetic database better knowledge of both the tectonic evolution of Western TMVB and fine characteristics of the Earth's Magnetic Field through the paleosecular analysis.

2. GEOLOGICAL SETTING AND SAMPLING

The Mascota Volcanic Field (MVF) is located within the Jalisco Block (western Mexico), between the TMVB and Sierra Cacoma. It lies south-west of the 250 km long Tepic-Zocoalo rift and north-west of the 65 km long Colima, two of the main known rift systems. MVF occupies the west part of the TMBV containing the volcanism mainly associated to the subduction process (*Bandy et al., 2001*).

The MVF presents one of the four volcanic fields (together with Los Volcanes, Ayutla, and Talpa) in the JB characterized by high potassium contents, slag cones, lava flows including absarokites, andesites, basaltic andesite minettes, basic hornblende lamprophyres and minettes in close spatial proximity to cones and flows of basaltic andesite and andesite (*Ownby et al., 2008*) and it is part of the alkaline volcanic fields within N-S to NE-SW (*Wallace and Carmichael; 1989*; *Lange and Carmichael, 1990*; *Righter and Carmichael, 1992*). MVF itself contains some deposits of Plio-Quaternary mafic rocks. The volcanism in the MVF is confined to the Talpa and Mascota grabens, with a few cones to the north that lie in an adjacent linear valley (*Carmichael et al., 1996*). The volcanism of Mascota appears to be the youngest of the four potassic volcanic fields in the JB (*Lange and Carmichael, 1991*; *Carmichael et al., 1996*), with reported ages of less than 1 Myr.

Volcanic rocks are distributed on an extensive area about 2000 km^2, which contains approximately 87 cones. *Ownby et al. (2008)* reported 35 $^{40}Ar/^{39}Ar$ dates revealing the eruptive history of the MVF. The oldest lavas are located in the southern sector, with dates between 2.4 Myr to 0.5 Myr. The younger lavas are mainly in the northern sector with dates predominantly < 0.5 Myr. In this study, 19 independent lava flows were sampled (Fig. 1.) The sample collection campaign was largely conditioned by detailed geochronology work of *Ownby et al., (2008)* since we tried to sample apparently fresh lava flows with available radiometric dates in unaltered and easy to Access outcrops. Sixteen flows were directly dated by *Ownby et al. (2008)* and range between 2268 kyr and 72 kyr. They are composed mainly by minette (MAS_01, MAS_09), absorkite (MAS_05, MAS_06, MAS_12 and MAS_19), basic hornblende lamprophyre (MAS_04, MAS_11, and MAS_14), basaltic andesite (MAS_03, Mas_13, MAS_15, MAS_16, MAS_17 and MAS_18) and andesite (MAS_10). Remaining three flows sampled are not dated by means of Ar-Ar systematics and may be described as follow: MAS_02 is a basic hornblende lamprophyre reported in the geological map of *Ownby et al. (2008)* to the south of MAS-419 and MAS-52, this flow was sampled due to the proximity with MAS_13 and MAS_14 and has not been reported previously; other flow sampled without age information is MAS_07 composed by minette and located close to MAS_06 and finally the site MAS_08 which is a lava flow composed of basaltic hornblende lamprophyre. Most of the studied flows are located in the MVF southern sector, near the Talpa Allende, with few flows located in the northern sector, near the San Sebastian area (Fig. 1), Seven out of 19 flows reported here were sampled in previous paleomagnetic studies by *Maillol and Bandy (1993)* and *Maillol et al. (1997)* (Fig. 1, MAS_09, MAS_11, MAS_14, MAS_16, MAS_15, MAS_17 and MAS_18). Eight to nine standard paleomagnetic cores were obtained from each independent cooling units and oriented using both magnetic and sun compasses.

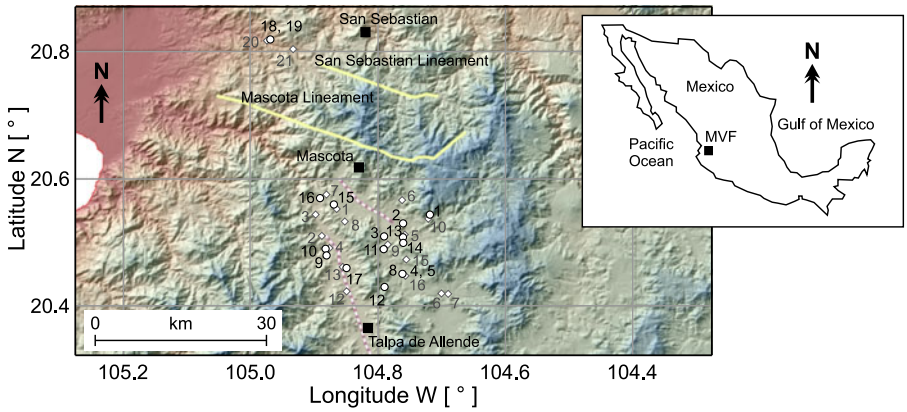

Fig. 1. Location of sampled lava flows from the Mascota Volcanic Field (MVF), Talpa de Allende and San Sebastian. The dots (black numbers) are the flows sampled in the present study, and the diamonds (grey numbers) represent the flows sampled by *Maillol and Bandy (1993)* and *Maillol et al. (1997)*.

3. MAGNETIC MEASUREMENTS

In order to identify the magnetic carriers responsible for the remanent magnetization and to obtain information about their paleomagnetic stability several rock-magnetic experiments were carried out. These experiments included:

- Thermomagnetic curves (temperature dependence of magnetization) helps to observe the proportional changes during the heating and cooling cycles and determine the Curie temperatures of the main magnetic minerals by means of the differential method described in *Tauxe (2002)*. These changes may involve the formation of new magnetic substances and different Curie points or changes in the phase. Continuous measurements in air were performed with a Curie balance from room temperature of about 22°C through 600°C.
- Magnetic hysteresis experiments were carried out to reveal the magnetic mineralogy. The hysteresis loops and associated Isothermal Remanent Magnetization (*IRM*) acquisition curves were measured using a Variable Field Translation Balance (VFTB). Measurements were carried out on whole-rock powdered specimens, and in each case, *IRM* acquisition and backfield curves were recorded first.
- Thermal and alternating field demagnetization techniques were applied to retrieve the Characteristic Remanent Magnetization (*ChRM*). All remanences were measured in the "Laboratorio Interinstitucional de Magnetismo Natural" (LIMNA), with JR-6A (AGICO Ltd.) spinner magnetometer.

The thermomagnetic curves provided information about magnetic mineralogy of samples through the Curie temperatures calculated using the differential method of *Tauxe (2002)*. This analysis revealed Curie temperatures between 350°C and 537°C indicating the presence of Ti-rich and Ti-poor titanomagnetites with moderate degrees of alteration due to heating (see representative examples in Fig. 2a,b). Some specimens, reveal coexistence Ti-rich titanomagnetites with almost pure magnetite (Fig. 2a). Only three flows, that were composed by basaltic hornblende lamprophyre and minette, show evidence of hematite (MAS_2, MAS_7 and MAS_8) yielding Curie temperatures close to 650°C (Fig. 2c), that were composed by basaltic hornblende lamprophyre and minette.

The hysteresis experiments provided simple curves pointing to the assemblages of pseudo-single-domain (PSD) ferromagnetic grains which are efficient in acquiring remanet magnetization and resistant to demagnetization exhibiting significant coercivity. Near to the origin, no evidence of wasp-waisted or potbellied behaviour is observed which suggests a very restricted ranges of coercivities for the ferromagnetic (s.l.) fractions (*Dunlop, 2002*; Fig. 2), and discarded the presence of two or more distinct coercivity population (*Roberts et al., 1995*; *Tauxe et al., 1996*). The isothermal remanence (*IRM*) acquisition curves are also sensitive to the magnetic mineralogy in terms of concentration and grain size properties. The analysis of coercivity spectra shows the correspondence of the magnetic saturation with the sample magnetic mineralogy. Most samples show

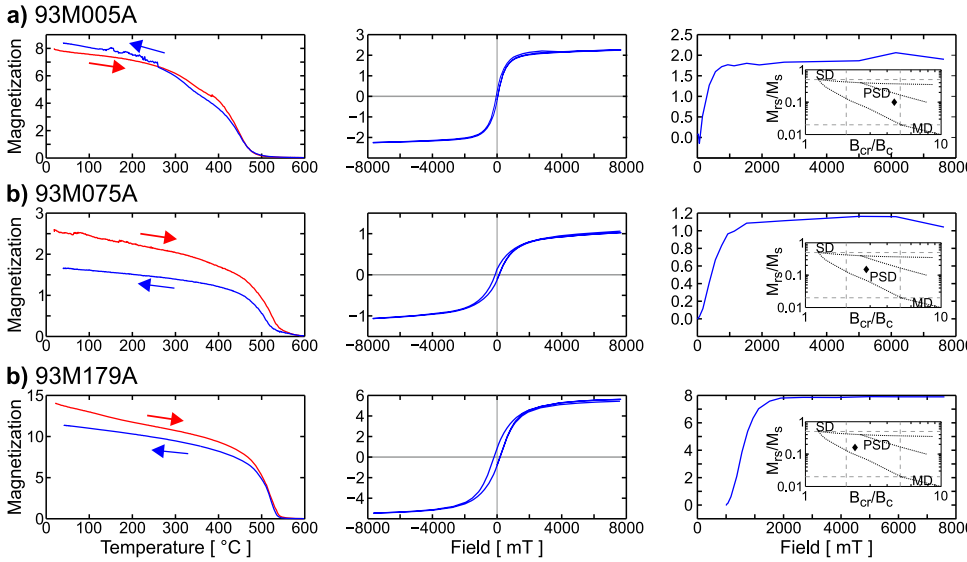

Fig. 2. Temperature dependence of magnetization (in 10^{-5} Am^2kg^{-1}), hysteresis loops (magnetization in 10^{-4} Am^2/kg) and curves of acquisition of isothermal remanent magnetization (*IRM*, in 10^{-5} Am^2/kg) of **a)** sample 93M005A from MAS_01, **b)** sample 93M075A from MAS_09, **c)** sample 93M179 from MAS_19. Insets show corresponding Day diagrams (B_{cr} - coercivity of remanence, B_c - coercive force, M_s - saturation magnetization, M_{rs} - saturation remanence, SD - single-domain, PSD - pseudo-single-domain, SP - super-paramagentic, MD - multi-domain).

saturation at about 300 mT applied magnetic field, which indicates presence of ferrimagnetic phases with moderate coercivity as may be expected from magnetite and titanomagnetite grains (*Tauxe, 2002*).

The initial stage of the measurement of the natural remanent magnetization (*NRM*) was achieved for five different specimens (pilot samples) from each of the 19 flows and were subjected to detailed thermal (two specimens) and alternating field demagnetization (AF, three specimens) in order to choose the most suitable demagnetization method for this study. An ASC TD-48 furnace was used during the thermal treatment from 50°C up to 560°C, while a Molspin AF-demagnetizer allowed demagnetizations starting from 5 mT up to 95 mT. The analysis of these pilot tests showed that AF demagnetization was more efficient (Fig. 3a–d) observed in 57 pilot samples. However, about 40 samples were thermally demagnetized with excellent results (Fig. 3d,f). All remaining samples were demagnetized using alternating fields yielding Median Destructive Fields (*MDF*) ranging from 25 mT to 40 mT, as should be expected from the pseudo-single domain ferromagnetic grains.

The remanence component directions and angular dispersion parameters for each one of the specimens and the paleomagnetic site-mean directions were determined by the

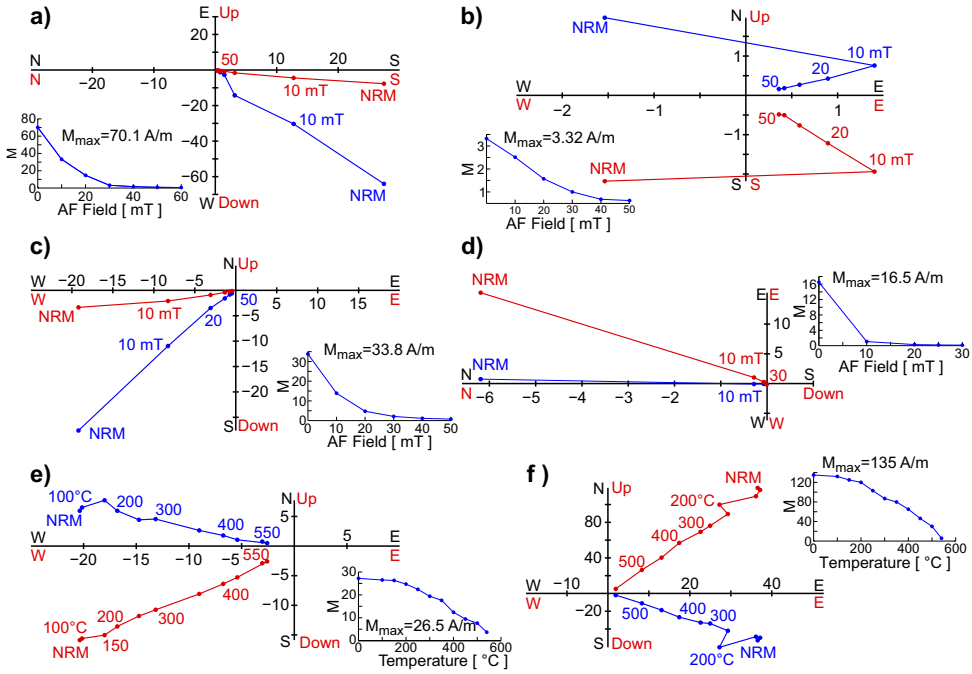

Fig. 3. Representative examples of orthogonal vector plots illustrating either alternative field or thermal treatments for representative samples: **a)** 93M020A from the flow MAS_03, **b)** 93M032A from the flow MAS_04, **c)** 93M053A from the flow MAS_06, **d)** 93M107A from the flow MAS_13, **e)** 93M120A from the flow MAS_14, and **f)** 93M136A from the flow MAS_15. *M* - magnetization.

method of the principal component analysis (*Kirschvink, 1980*) and Fisher statistics (*Fisher, 1953*). Although all these 8 samples per sites were demagnetized using either alternating field or thermal treatments, in average 5 to 6 samples were used for site-mean paleodirections determination. Remaining samples were rejected from the analysis because their maximum angular deviation (*MAD*) exceeded 2°. In some cases, we observe a well-defined *ChRM* direction, accompanied by secondary components easily removed (Fig. 3b,e,f), and in a few samples we detected a simple component accompanied by a negligible viscous overprint (Fig. 3a,c,d). The mean paleodirections determined for all sites in this study are quite precisely determined since for most cases the values of the 95% confidence angle α_{95} are less than 10°. They were combined with previous paleodirections reported form studies of the same area (Table 1; *Maillol et al., 1997*) in order to increase the robustness of paleomagnetic analysis.

4. RESULTS AND DISCUSSION

The 19 paleodirections obtained (16 of them directly dated by means of $^{40}Ar/^{39}Ar$ systematics), were distributed in ten paleodirections for the Brunhes chron and six paleodirections to the Matuyama chron (Fig. 4) while three undated flows (MAS_02, MAS_07 and MAS_08) belong to Brunhes chron judged from their magnetic polarity (Table 1). The evidence of transitional directions was detected for the flow MAS_15 (Table 1) which may correspond to the Levantine excursion (360–370 kyr) an unnamed event between 400–420 kyr (*Laj and Channell, 2007*). Both apparent transitional events are poorly defined (*Ryan, 1972*; *Singer et al., 2002*), although, the Levantain event was already reported by *Rodríguez et al. (2006)* in lava flows associated to the TVF. It is interesting to note that same flow, previously studied by *Maillol and Bandy (1993)* (Site MAS-1), also yielded the anomalous paleodirections (Table 1 and Fig. 4b). Both determinations are well constrained based on 5 samples for the present study while *Maillot et al. (1993)* reported analysis carried out on 8 paleomagnetic cores.

The identification of low technical quality data and transitional events are required to correctly characterize the PSV (*Johnson et al., 2008*), for this reason the paleomagnetic data with $N \leq 4$, $\alpha_{95} \geq 10°$, and virtual geomagnetic pole latitude $VGP_{lat} < 60°$ were omitted for further analysis. As a result, eleven paleodirections yielded mean paleodirection with mean declination $D_m = 359.2°$, mean inclination $I_m = 39.6°$, corresponding precission parameter $k = 17.96$ and 95% confidence angle $\alpha_{95} = 9.8°$.

The previous study performed by *Maillol et al. (1997)* reported data from 16 lava flows, which meet the basic selection criteria (Table 1, Fig. 4) yielding a mean direction determined by $D_m = 354.5°$, $I_m = 36.3°$, $k = 22.04$ and $\alpha_{95} = 7.9°$ for $N = 14$, a combined paleomagnetic direction based on 22 independent flows yield a mean direction determined by $D_m = 356.8°$, $I_m = 39.9°$, $k = 22$ and $\alpha_{95} = 6.4°$.

The selected paleodirections span two polarity chrons (Table 2):

1. The Brunhes chron (approx. 780 kyr to present) is represented by 17 flows yielding $D_{Bm} = 354.7°$, $I_{Bm} = 40.1°$, $k = 19.8$ and $\alpha_{95} = 7.6°$.
2. The Matuyama chron (between 780 kyr and 2.46 Myr) is represented by five flows with a mean paleodirection $D_{Mm} = 0.8°$, $I_{Bm} = 39.4°$, $k = 30.3$ and $\alpha_{95} = 11.4°$.

Table 1. Results of flow mean paleodirections for Mascota Volcanic Field lavas. Site: Names of the sample sites as described in *Ownby et al. (2008)*; *Lat*, *Long*: geographical latitude and longitude of the sampled sites; *D* and *I*: flow-mean declination and inclination; *k* and α_{95}: precision parameter and 95% confidence angle (*Fisher, 1953*); *N*: number of specimens used for the mean calculation; Age: Ar-Ar ages of the flows in ka; σ_{age}: dispersion of the age provided by the radiometric dating (Ar-Ar) in kyr; VGP_{lon} and VGP_{lat}: virtual geomagnetic pole latitude and longitude, respectively; A_{95} and *K*: precision parameters of the VGPs; Ref: 1 - this study, 2 - *Maillol and Bandy (1993)* and *Maillol et al. (1997)*.

Site	*Lat* [°]	*Long* [°]	*D* [°]	*I* [°]	*k*	α_{95} [°]	*N*	Age [kyr]	σ_{age} [kyr]	VGP_{lon} [°]	VGP_{lat} [°]	Ref
MAS_01	20.54	104.72	355.20	54.70	76.20	8.70	6	73	14	269.69	74.72	1
MAS-5	20.51	104.76	340.70	20.10	122.50	4.70	9	163	13	169.02	68.84	2
MAS_14	20.51	104.76	339.46	32.42	46.71	10.24	4	163	13	189.76	70.39	1
MAS-7	20.58	104.88	3.30	35.30	181.20	5.70	5	166	22	33.52	86.72	2
MAS-6	20.50	104.76	356.80	38.20	422.40	2.70	8	196	11	213.45	86.86	2
MAS_16	20.57	104.89	356.36	33.90	44.80	11.20	5	248	39	165.28	86.03	1
MAS-20	20.82	104.97	2.60	34.60	198.00	3.40	10	257	24	50.70	86.97	2
MAS_18	20.82	104.97	2.71	36.40	90.61	5.19	8	257	24	27.46	87.40	1
MAS-1	20.55	104.87	1.90	–3.60	221.20	3.70	8	385	35	279.88	-67.57	2
MAS_15	20.56	104.87	56.50	4.90	326.30	6.50	5	385	35	25.31	32.10	1
MAS-13	20.46	104.86	14.00	18.80	878.30	1.70	9	497	19	51.46	72.72	2
MAS_17	20.46	104.85	2.80	5.60	348.20	4.20	5	497	19	95.70	72.14	1
MAS_19	20.82	104.97	4.68	22.39	618.16	1.99	8	568	30	82.44	77.96	1
MAS_06	20.42	104.70	7.90	50.00	68.20	9.50	5	576	8	317.55	77.43	1
MAS_04	20.49	104.79	331.78	55.58	142.30	4.18	8	635	11	233.21	60.82	1
MAS_05	20.49	104.79	354.80	66.70	31.50	11.90	5	661	8	277.80	60.93	1
MAS-3	20.54	104.90	341.30	19.80	331.30	2.70	10	<780	NA	167.83	69.25	2
MAS-8	20.53	104.35	359.50	47.40	397.00	2.60	9	<780	NA	281.20	81.99	2
MAS-9	20.50	104.79	344.60	55.00	54.00	7.10	9	<780	NA	246.07	69.79	2
MAS-10	20.54	104.72	345.70	18.80	42.40	8.00	9	<780	NA	158.55	72.44	2
MAS-15	20.47	104.76	347.90	65.00	529.10	2.40	8	<780	NA	267.20	61.71	2
MAS-21	20.81	104.93	352.80	31.50	39.30	7.80	10	<780	NA	167.17	82.22	2
MAS_02	20.53	104.76	300.00	–52.10	70.74	11.00	4	<780	NA	123.40	11.18	1
MAS_07	20.42	104.70	14.80	51.70	52.30	9.60	6	<780	NA	329.64	72.21	1
MAS_08	20.50	104.76	338.20	52.30	62.20	9.70	5	780	NA	231.85	66.99	1
MAS_10	20.49	104.88	174.80	–19.10	29.30	14.30	5	915	48	130.81	78.21	1
MAS_12	20.43	104.79	196.90	–32.30	65.20	8.60	4	1416	8	22.20	73.77	1
MAS-12	20.42	104.85	179.80	–49.00	442.50	2.30	10	1597	16	283.80	80.51	2
MAS_11	20.46	104.85	352.69	42.96	415.80	3.60	6	1597	16	229.98	81.89	1
MAS-2	20.51	104.89	180.90	–50.00	280.00	3.10	9	1613	6	289.21	79.69	2
MAS_03	20.51	104.79	97.05	61.69	13.24	22.24	3	1618	37	332.20	8.87	1
MAS-4	20.49	104.88	173.30	–20.50	248.90	3.20	9	2159	6	138.95	78.19	2
MAS_09	20.48	104.88	172.06	–22.82	31.39	9.44	7	2159	6	147.63	78.51	1
MAS_13	20.45	104.76	355.10	64.60	48.77	12.30	4	2354	42	277.14	63.37	1
MAS-16	20.45	104.76	168.00	26.40	635.90	2.20	8	2354	42	304.66	–53.65	2

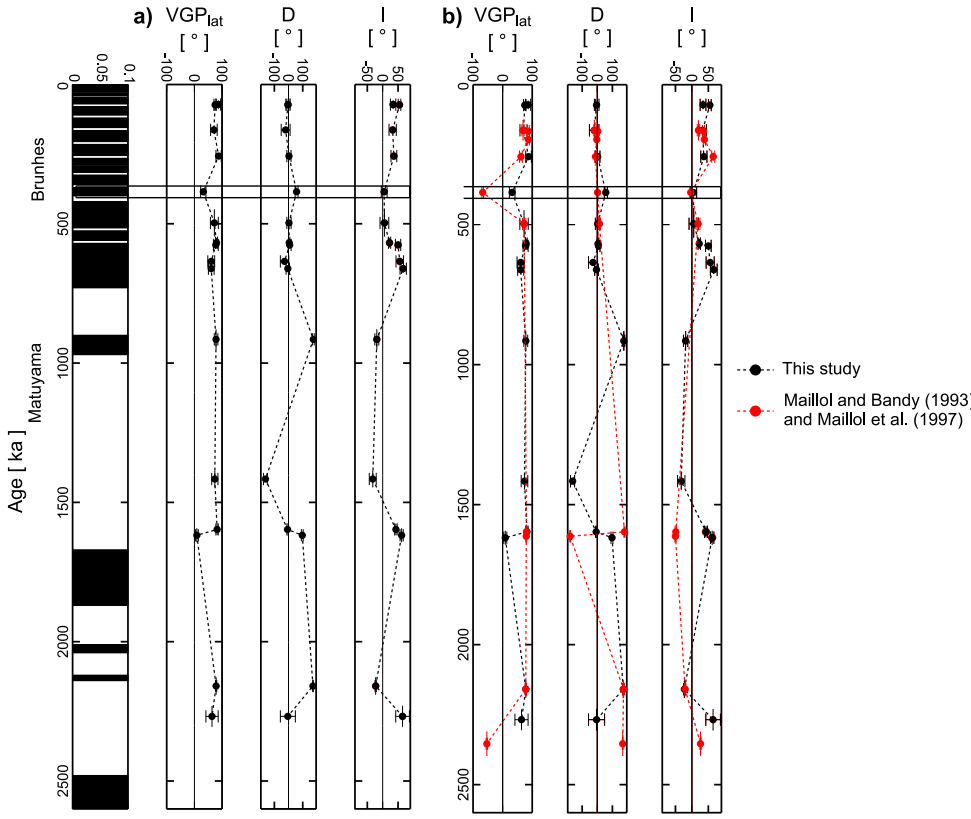

Fig. 4. Mean paleomagnetic virtual geomagnetic pole latitude (VGP_{lat}), declination (D) and inclination (I) versus age for the flows of the Mascota Volcanic Field, Talpa and San Sebastian. **a)** Data from this study, and **b)** comparison with data of *Maillol and Bandy (1993)* and *Maillol et al. (1997)* (see text for more details).

Based on this analysis, we conclude that the most representative direction for the MVF is the mean paleodirection that involve the 22 lava flows (Table 2, Fig. 5). These directions are practically undistinguishable from the expected directions retrieved from both *Besse and Courtillot (2002)* and *Torsvik et al. (2012)* reference poles (Fig. 5) with difference observed in the flattening parameter $F_{BC} = -5.09 \pm 5.97$ and rotation parameter $R_{BC} = -0.31 \pm 7.0$, and $F_T = -3.00 \pm 5.91$ and $R_T = -2.01 \pm 7.0$, respectively. The mean paleodirection was compared with the Geomagnetic Axial Dipole (GAD) direction for the geographic coordinate of Mascota at 20°32′N, 104°49′W and indicate a slight difference $\Delta D = 3.92°$ and $\Delta I = 3.19°$. This is compared with the inclination anomaly ΔI as a function of latitude, compiled by *Johnson el al. (2008)* (Fig. 6). Moreover, the same paleodirections were compared with the study of *Lawrence et al. (2006)*, which performed an analysis from several areas showing that the VGP dispersion parameters for about

Table 2. Comparison of paleomagnetic analysis of this study (Ref. 1) with the previous work by *Maillol et al. (1997)* (Ref. 2) and composite (22 flows) dataset, to compare the distribution after removal of the data corresponding to virtual geomagnetic pole latitudes lower than cutoff angle (Cutoff). D - mean declination, I - mean inclination, k, α_{95} - the respective Fisher quality parameters, N -the number of data used, VGP_{Long}, VGP_{Lat} - the virtual geomagnetic pole, K, A_{95} – the respective quality parameters, and S_B - the angular standard deviation.

Ref.	Cutoff [°]	D [°]	I [°]	k	α_{95} [°]	N	VGP_{Long} [°]	VGP_{Lat} [°]	K	A_{95} [°]	S_B [°]
1	60	359.22	39.61	17.96	9.95	11	264.37	86.47	23.37	8.73	16.82
2	60	354.52	36.33	22.04	7.96	14	207.38	84.86	30.62	6.76	13.97
All	60	356.08	39.99	22.02	6.36	22	239.05	84.78	27.23	5.71	16.49
All. B.	60	354.66	40.12	19.78	7.63	17	232.85	83.58	24.4	6.87	17.75
All. M.	60	360.78	39.35	30.27	11.37	5	299.59	87.35	41.82	9.68	12.89
All Rad	60	359.23	38.01	25.21	7.45	14	256.17	87.91	31.62	6.65	14.65

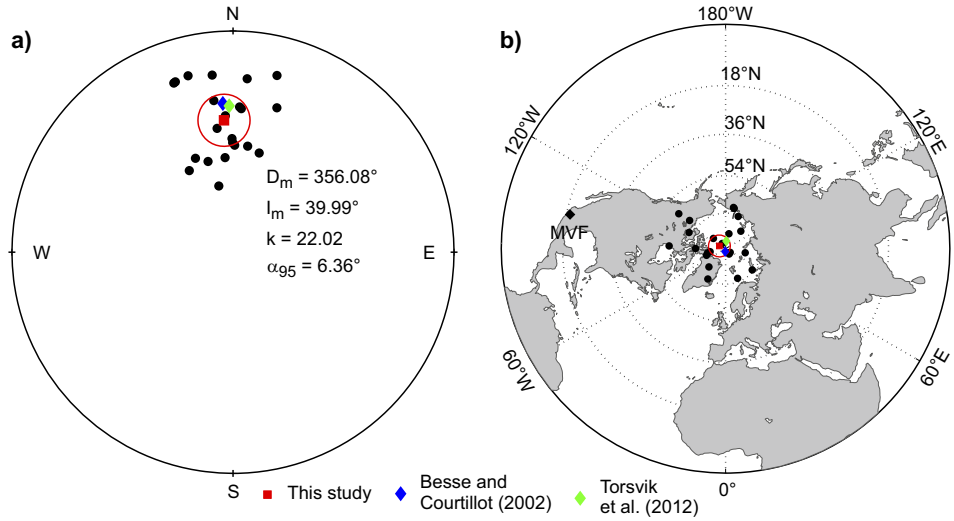

Fig. 5. **a)** Equal area projection of the mean paleomagnetic directions obtained in this study. **b)** Projection of the virtual geomagnetic poles (VGPs) obtained in this study (VGP_{lat} = 84.78°, VGP_{lon} = 239.06°, precision parameter K = 27.23, 95% confidence angle A_{95} = 5.71°) together with reference paleomagnetic poles calculated from the stable North America (*Besse and Courtillot, 2002*; *Torsvik et al., 2012*).

20°N latitudes are consistent with the present study. This comparation test also indicates that the mean inclination difference is also smaller during the Matuyama than Brunhes (Table 2), in agreement with the results presented for México by *Lawrence et al. (2006)*.

A reversal test applied to the site mean paleodirections is positive yielding type C (Fig. 7, Table 3) as derived from calculations reported in *McFadden and McElhinny (1990)*. The angular standard deviation (often called angular dispersion) of the VGPs

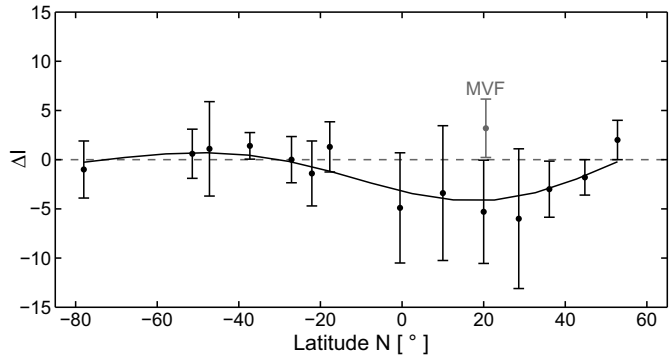

Fig. 6. Inclination anomaly Δ*I* versus latitude for normal and reverse data compiled by *Johnson et al. (2008)* (dots) with a 95% confidence intervals (error bars), and best-fit two-parameter zonal field model (solid line). MVF indicates the inclination anomaly for the Mascota Volcanic Field with respect to the mean geographic average latitude.

yields a value of $S_B = 16.49°$ with the lower confidence limit $S_{BL} = 15.13°$ and the upper confidence limit $S_{BU} = 18.10°$ (*Cox, 1969*). The value of the angular dispersion matches with the Model G of *Johnson et al. (2008)* and which gives a value of about 16° for the latitudes around 20° (Fig. 8). This however is true for Bruhnes chron while little bit higher dispersion is expected for the Matuyama chron. It should be noted that the model of *Johnson et al. (2008)* was developed using a criteria for data selection very similar to present study. Some differences observed between the Model G of *McFadden et al. (1997)* and TK03 of *Tauxe and Kent (2004)* is probably due to the fact that the Model G used lest strict selection criteria while TK03 is based made on different materials than volcanic flows.

The dispersion parameters obtained in present investigation is compatible to other studies carried out along the central and western Mexico (*Mejia et al., 2005*; *Conte-Fasano et al., 2006*; *Ruiz-Martinez et al., 2010*). The same is true to sites belonging to similar latitudes, as Réunion, the South Pacific and Hawaii (*Lawrence et al., 2006*). The possible occurrence of Levantine geomagnetic event in MVF lavas is supported by two independent nearby lava flows belonging to Tequila Volcanic Field dated as 362 ± 13 and 354 ± 5 kyr respectively yielding transitional paleodirections (*Rodríguez et al., 2006*). Levantine excursion at about 360 kyr is classified in *Singer et al. (2002)* geomagnetic instability time scale as a poorly defined excursion (*Ryan, 1972*). Some evidence of this short event was also reported by *Torii et al. (1974)* from the Osaka area (370–380 kyr) and *Negrini et al. (1988)* from the Summer Lake (360–370 kyr).

5. CONCLUSIONS

Detailed rock-magnetic experiments, which included continuous thermomagnetic curves, isothermal remanent magnetization and hysteresis measurements, indicate that ferrimagnetic phases with low to moderate coercivities corresponding to both Ti-poor

Table 3. Results of the reversal test (*McFadden and McElhinny, 1990*) for flows of Mascota Volcanic Field (MVF), Talpa and San Sebastian, using all selected paleodirections to obtain the critical angle, which is useful to classify different distributions. Observed angle is the angle between the normal and reversed distribution for; *Rc* is critical value associated with the critical angle; *k*1 and *k*2 are precision values associated with the normal and reversed distribution, respectively.

Distributions Studied	Critical Angle [°]	Observed Angle [°]	*Rc*	*k*1	*k*2	Classification
Maillol et al. (1997)	21.88	5.47	13.25	20.35	22.71	indeterminate
This study	22.03	19.83	15.10	17.95	34.15	indeterminate
All	17.75	6.61	20.91	20.98	24.47	positive reversal test

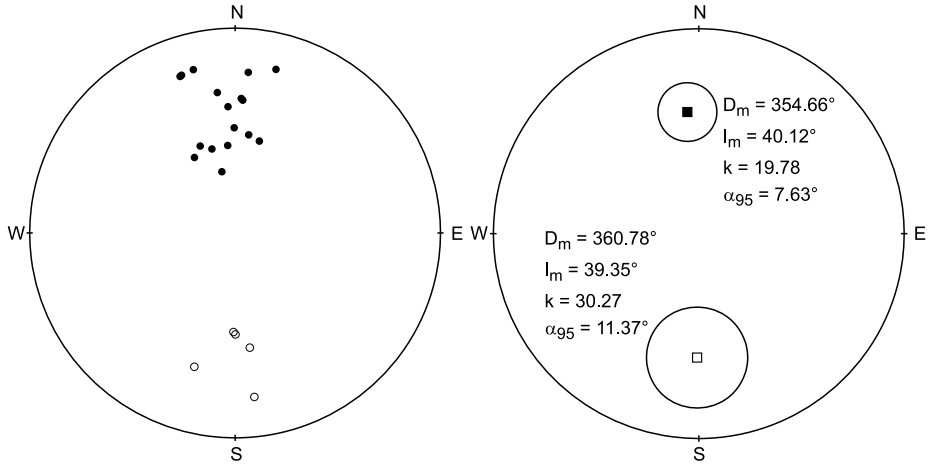

Fig. 7. Results of the distribution with positive reversal test (*McFadden and McElhinny, 1990*) listed in Table 3, showing the normal (full symbols) and reversed (blank symbols) distribution of directions, the mean declination (D_m) and inclination (I_m) and the corresponding quality parameters (k and α_{95}) for the Mascota Volcanic Field lava flows.

(almost magnetite phase) and Ti-rich titanomagnetites are responsible of magnetization in majority of cases.

The present study increased the number of high standart paleomagnetic data from the Jalisco Block adding nineteen radiometrically dated sites which allwed to increase the robustness of existing data from the western part of the Trans-mexican Volcanic Belt during Plio-Pleistocene.

Thirteen flows correspond to the Brunhes chron, one of them exhibits transitional directions, while the remaining six sites belong to the Matuyama chron. The combined paleomagnetic dataset, supported by positive reversal test, indicate no paleomagnetically detectable vertical-axis rotations in the study area.

The evidence of one transitional directions was detected, which may correspond to the Levantine excursion (360–370 kyr) or unnamed event between 400–420 kyr.

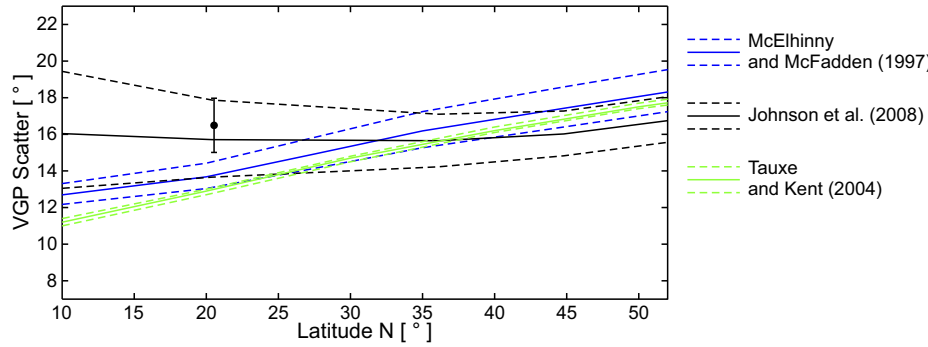

Fig. 8. Comparison of three models of scatter of virtual geomagnetic pole as a function of the latitude for the last 5 Myr. The dot with error bar represents the Mascota Volcanic Field data.

Acknowledgments: The authors are thankful for the financial support provided by UNAM-PAPIIT IN101717. M. Cervantes is grateful for financial support given by UNAM-PAPIIT-IA104215

References

Bandy W.L., Urrutia-Fucugauchi J., McDowell F.M. and Morton-Bermea O., 2001. K-Ar ages of four mafic lavas from the Central Jalisco Volcanic Lineament: Supporting evidence for NW migration of volcanism within the Jalisco block, western Mexico. *Geof. Int.*, **1**, 259–269.

Besse J. and Courtillot V., 2002. Apparent and true polar wander and the geometry of the geomagnetic field in the last 200 Myr. *J. Geophys. Res.*, **107**, 2469, DOI: 10.1029 /2000JB000050.

Carmichael I.S.E., Lange R.A. and Luhr J.F., 1996. Quaternary minettes and associated volcanic rocks of Mascota, western Mexico: a consequence of plate extension above a subduction modified mantle wedge. *Contrib. Mineral. Petrol.*, **124**, 302–333.

Conte-Fasano G., Urrutia-Fucugauchi J., Goguitchaichivili A. and Morales-Contreras J., 2006. Low-latitude paleosecular variation and the time-averaged field during the late Pliocene and Quaternary-paleomagnetic study of the Michoacán-Guanajuato volcanic field, Central Mexico. *Earth Planets Space*, **58**, 1359–1371, DOI: 10.1186/BF03352632.

Dunlop D.J., 2002. Theory and application of the Day plot (Mrs/Ms versus Hcr/Hc) 1. Theoretical curves and tests using titanomagnetite data. *J. Geophys Res.*, **107**, 2056, DOI: 10.1029 /2001JB000486.

Ferrari L., 2000. Avances en el conocimiento de la Faja Volcánica Transmexicana durante la última época (Advances in the understanding of the Trasnmexican Volcanic Belt during the last period). *Bol. Soc. Geol. Mex.*, **V**, 84–92.

Fisher R.A., 1953. Dispersion on a sphere. *Proc. R. Soc. London A*, **217**, 295–305.

Johnson C.L and Constable C.G., 1995. The time-average field record by lava flows over the past 5 Myr. *Geophys. J. Int.*, **122**, 489–519.

Johnson C.L and Constable C.G., 1998. Persistently anomalous Pacific geomagnetic fields. *Geophys. Res. Lett*., **25**, 1011–1014.

Johnson C.L., Constable C.G., Tauxe L., Barendregt R., Brown L.L., Coe R.S., Layer P., Mejia V., Opdyke N.D., Singer B.S., Staudigel H. and Stone D.B., 2008. Recent investigations of the 0–5 Ma geomagnetic field recorded by lava flows. *Geochem. Geophys. Geosyst.*, **9**, 1525–2027, DOI: 10.1029/2007gc001696.

Kirschvink J.L., 1980. The least-square line and plane and analysis of paleomagnetic data. *Geophys. J. Int.*, **62**, 699–718, DOI: 10.1111/j.1365-246X.1980.tb02601.x.

Laj C. and Channel J.E.T., 2007. Geomagnetic excursions. In: Kono M. (Ed.), *Geomagnetism*. Treatise on Geophysics 5. Elsevier Science, Amsterdam, The Netherlands.

Lange R.A. and Carmichael I.S.E., 1990. Hydrous basaltic andesites associated with minette and related lavas in Western Mexico. *J. Petrol.*, **31**, 1225–1259, DOI: 10.1093/petrology /31.6.1225.

Lange R.A. and Carmichael I.S.E., 1991. A potassic volcanic front in western Mexico: The lamprophyric and related lavas of San Sebastian. *Geol. Soc. Am. Bull.*, **103**, 928–940.

Lawrence K.P. and Constable C.G., 2006. Paleosecular variation and the average geomagnetic field at ±20° latitude. *Geochem. Geophys. Geosyst.*, **7**, DOI: 10.1029/2005GC001181.

Luhr J.F., Nelson A.S., Allan F.J. and Carmichael I.S.E., 1985. Active rifting in southwestern Mexico: Manifestations of an incipient eastward spreading-ridge jump. *Geology*, **13**, 54–57, DOI: 10.1130/0091-7613(1985)13<54:ARISMM>2.0.CO;2.

Maillol J.M. and Bandy W.L., 1993. Paleomagnetism of the Talpa de Allende and Mascota grabens western Mexico: A preliminary Report. *Geofis. Int.*, **33**, 153–160.

Maillol J.M., Bandy W.L. and Ortega Ramírez J., 1997. Paleomagnetism of Plio-Quaternary basalts in the Jalisco block, western Mexico. *Geofis. Int.*, **36**, 0 (http://www.redalyc.org/pdf /568/56836103.pdf).

McElhinny M.W., McFadden P.L. and Merrill R.T., 1996. The time-average paleomagnetic field 0–5 Ma. *J. Geophys. Res.*, **101**, 25007–25027, DOI: 10.1029/96JB01911.

McElhinny M.W. and McFadden P.L., 1997. Paleosecular variation over the past 5 Myr based on a new generalized database. *Geophys. J. Int.*, **131**, 240–252, DOI: 10.1111/j.1365-246.X.1997.tb01219.x.

McFadden P.L. and McElhinny M.W., 1990. Classification of the reversal test in paleomagnetism. *Geophys. J. Int.*, **103**, 725–729, DOI: 10.1111/j.1365-246X.1990.tb05683.x.

Mejia V., Böhnel H., Opdyke N.D., Ortega-Rivera M.A., Lee J.K.W. and Aranda-Gomez J.J., 2005. Paleosecular variation and time-averaged field recorded in Late Pliocene–Holocene lava flows from Mexico. *Geochem. Geophys. Geosyst.*, **6**, DOI: 10.1029/2004GC000871.

Merril R.T. and McElhinny M.W., 1985. *The Earth's Magnetic Field. Its History, Origin and Planetary Perspective*. Academic Press, London, U.K., ISBN: 978-0124912427.

Negrini R.M., Verosub K. and Davis O., 1988. The middle to late Pleistocene geomagnetic field recorded in fine-grained sediments from Summer lake, Oregon and Double Hot Springs, Nevada, USA. *Earth Planet. Sci. Lett.*, **87**, 19–38, DOI: 10.1016/0012-821X(88)90073-8.

Ownby S.E., Lange R.A. and Hall C.M., 2008. The eruptive history of the Mascota volcanic field, western Mexico: Age and volume constraints on the origin of andesite among a diverse suite of lamprophyric and calc-alkaline lavas. *J. Volcanol. Geotherm. Res*., **117**, 1077–1091.

Prévot M., Mankinen E.A., Gromme S.C. and Coe R.S., 1985. How the geomagnetic field vector reverses polarity. *Nature*, **316**, 230–234, DOI: 10.1038/316230a0.

Rigthter K. and Carmichael I.S.E., 1992. Hawaiites and related lavas in the Atenguillo graben, western Mexican Volcanic Belt. *Geol. Soc. Am. Bull*., **104**, 1592–1607, DOI: 10.1130/0016-7606(1992)104<15:HARLIT>2.3.CO;2.

Rodríguez C.M., Goguitchaichvili A., Calvo-Rather M., Morales C.J., Alva-Valdivia L.A., Rosa E.J., Urrutia-Fucugauchi J. and Delgado G.H., 2006. Paleomagnetism of the Pleistocene Tequila Volvanic Field (Western Mexico). *Earth Planets Space*, **58**, 1349–1358, DOI: 10.1186/BF03352631.

Roberts A.P., Cui Y. and Verosub K.L., 1995. Wasp-waisted hysteresis loops: mineral magnetic characteristics and discrimination of components in mixed magnetic systems. *J. Geophys. Res.*, **100**, 17909–17924, DOI: 10.1029/95JB00672.

Ruiz-Martinez V.C., Urrutia-Fucugauchi J. and Osete M.L., 2010. Paleomagnetism of the Western and Central sectors of the Trans-Mexican volcanic belt-implications for the tectonic rotations and paleosecular variation in the paste 11 Ma. *Geophys. J. Int*., **180**, 577–595, DOI: 10.1111 /j.1365-246X.2009.04447.x.

Ryan W.B., 1972. Stratigraphy of late Quaternary sediments in the eastern Mediterranean. In: Stanley D.J. (Ed.), *The Mediteranean Sea: A Natural Sedimentation Laboratory*. Dowden, Hutchinson & Ross, Stroudsburg, PA.

Schneider D.A. and Kent D.V., 1990. The time-average paleomagnetic field. *Rev. Geophys*., **28**, 71–96, DOI: 10.1029/RG28i001p00071.

Singer B.S., Relle M.K., Hoffman K.A., Battle A., Laj C., Guillou H. and Carracedo J., 2002. Ar/Ar ages from transitionally magnetized lavas on La Palma, Canary Islands, and the geomagnetic instability timescale. *J. Geophys. Res*., **107**, 2307, DOI: 10.1029/2001JB001613.

Tauxe L., Mullender T.A.T. and Pick T., 1996. Potbellies, wasp-waists, and superparamagnetism in magnetic hysteresis. *J. Geophys. Res*., **101**, 571–583, DOI: 10.1029/95JB03041.

Tauxe L., 2002. *Paleomagnetic Principles and Practice*. 1st Edition. Kluwer Academic Publisher, Dordrecht, The Netherlands.

Tauxe L. and Kent D.V., 2004. A simplified statistical model for the geomagnetic field and detection of shallow bias in paleomagnetic inclinations: was the ancient magnetic field dipolar? In: Channell J.E.T., Kent D.V., Lowrie W. and Meert J.G. (Eds), *Timescales of the Paleomagnetic Field*., American Geophysical Union, Washington, D.C., DOI: 10.1029 /145GM08.

Torii M., Yoshikawa S. and Itihara M., 1974. Paleomagnetism in the water-laid volcanic ash layer in the Osaka Group, Sennan and Senpoku hills, southwest Japan. *Rock Magn. Paleogeophys.*, **2**, 34–37.

Torsvik T.H., Van der Voo R., Preeden U., Mac Niocail C., Steinberger B., Hinsbergen B., Doubrovine P.V., van Hinsbergen D.J.J., Domier M., Gaina C., Tohver E., Meert J.G., McCausland P.J.A. and Cocks L.R.M., 2012. Phanerozoic polar wander, palaeogeography and dynamics. *Earth Sci. Rev.*, **114**, 325–368, DOI: 10.1016/j.earscirev.2012.06.007.

Wallace P. and Carmichael I.S.E., 1989. Minette lavas and associated leucitites from the western front of the Mexican Volcanic belt: Petrology, chemistry, and origin. *Contrib. Mineral. Petrol.*, **103**, DOI: 470-492, 10.1007/BF01041754.

Wilson R.L., 1972. Palaeomagnetic differences between normal and reverse field sources, and the problem of far-side and right-handed pole positions. *Geophys. J. R. Astron. Soc*., **28**, 295–304.

Wilson R.L. and McElhinny M.W., 1974. Investigation of the large scale palaeomagnetic field over the past 25 million years: eastward shift of the Icelandic spreading ridge. *Geophys. J. R. Astron. Soc.*, **39**, 570–586.